Identification of a DNA aptamer that inhibits sclerostin's antagonistic effect on Wnt signaling

Ka To Shum*[1], Celine Chan*[1], C. M. Leung*, Julian A. Tanner*[2]

*Department of Biochemistry, University of Hong Kong, 21 Sassoon Road, Pokfulam, Hong Kong.

[1]These authors contributed equally to this work.

[2]To whom correspondence should be addressed (phone: +852 2819 9472; Fax: +852 28551254; e-mail: jatanner@hkucc.hku.hk**)**.

Short title: Aptamers against sclerostin.

Key words: sclerostin, sclerosteosis, isothermal titration calorimetry, SELEX, G-quadruplex, Wnt signaling.

SYNOPSIS

Sclerostin is an extracellular negative regulator of bone formation that is a recognised therapeutic target for osteoporosis therapy. Here, we perform DNA aptamer selection against sclerostin, then characterise aptamer-sclerostin binding and ability to inhibit sclerostin function in cell culture. We show that a selected DNA aptamer was highly selective for binding to sclerostin with affinities in the nanomolar range as determined by solid-phase assays and by isothermal titration calorimetry. Binding between sclerostin and the aptamer was exothermic and enthalpically driven. Circular dichroism confirmed that the aptamer had temperature-dependent parallel G-quadruplex characteristics. The aptamer was stabilised with 3' inverted thymidine to investigate efficacy at inhibiting sclerostin function in cell culture. The stabilised DNA aptamer showed potent and specific dose-dependent inhibition of sclerostin's antagonistic effect on Wnt activity using a reporter assay. Taken together, these studies present an alternative approach to inhibiting sclerostin function with therapeutic potential.

INTRODUCTION

Sclerostin is an extracellular protein secreted by osteocytes that acts to negatively regulate bone formation [1, 2]. Loss of function mutations in the gene coding for sclerostin, *SOST*, result in the congenital disease sclerosteosis, characterised by strong and dense bone [1-4]. As such, sclerostin has become a key target in the development of new therapeutics for the treatment of osteoporosis, and significant progress has been made in recent years with monoclonal antibodies that inhibit sclerostin function that are now in clinical trials [5-8].

Sclerostin is a member of the cystine-knot family including DAN, Cerberus, Caronte and Dante, often known as the DAN protein family. Typically these proteins act by binding to bone morphogenetic protein (BMP) and antagonising their functions [9, 10]. Whilst sclerostin was observed to bind to BMPs, it is most likely that sclerostin mainly acts by binding directly to low density lipoprotein receptor-related protein 4, 5 and 6 (LRP 4/5/6), thereby antagonising canonical Wnt signaling [11-14]. Frizzled and LRP 5/6 are receptors for transduction of canonical Wnt signaling leading to stabilisation of β-catenin and regulation of gene transcription by lymphoid enhancing factor (LEF1) and T-cell factors (TCF) [15]. Defects in this signaling pathway have been frequently implicated in congenital skeletal diseases, for example loss of function mutations in LRP5 are responsible for human osteoporis-pseudoglioma syndrome and gain of function mutations result in a high bone mass phenotype [16, 17].

As the most common treatments for osteoporosis such as oral bisphosphonates are antiresorptive rather than anabolic, sclerostin was proposed to be a potentially superior therapeutic target. Monoclonal antibodies against sclerostin showed complete reversal of oestrogen deficiency-induced bone loss in a mouse model [18], and were able to inhibit colitis in a mouse model of chronic colitis [19]. Dose-dependent increases in bone formation, bone mineral density and bone strength were observed in a cynomolgus

monkey study [20]. In rats, monoclonal antibodies showed bone anabolic effects at bone marrow sites [21], and were also shown to enhance metaphyseal bone healing [22]. The first human study using a sclerostin monoclonal antibody showed general safety and tolerability with increases in a number of bone formation markers [7], and clinical trials with regards to efficacy for increased bone formation are ongoing [23].

Whilst it is now clear that sclerostin is a particularly promising target for increasing bone formation, there are a number of competing strategies, besides monoclonal antibodies, that might be used to inhibit sclerostin function [24]. Nucleic acid aptamers selected by *in vitro* evolution are one alternative approach that have similar affinities and specificities to monoclonal antibodies, with potential benefits of scalable and modifiable chemical synthesis, small in size and low immunogenicity [25-27]. Indeed, in the recent human sclerostin monoclonal antibody study, six subjects in the higher dose groups did develop neutralising antibodies against the therapy [7]. Aptamers have been clinically proven by pegaptanib (marketed as Macugen), an aptamer-based drug used in the treatment of age-related macular degeneration [28] that targets the extracellular protein VEGF thereby inhibiting its interaction with its receptors VEGFR1 and VEGFR2 [29].

In an effort to identify DNA-aptamer inhibitors of sclerostin, we have screened a DNA aptamer library with a 30-nt variable region. Using this approach, we identified a family of parallel G quadruplex aptamers that potently and specifically bind to sclerostin by independent assays. After stabilisation, one aptamer showed dose-response potent inhibition of sclerostin-mediated antagonism of Wnt signaling in cell culture.

EXPERIMENTAL

Source of DNA and cloning. The cDNA of SOST was obtained form *Mus musculus* 6 days neonate head cDNA, clone: 5430411E23 (RIKEN; Japan). The coding region of SOST was amplified by PCR, using TaKaRa LA taq polymerase (RR002M; TaKaRa) with the forward primer 5'-GTATGTATGAATTCATGCATGCAGCCCTCACTAGCCCC-3' and the reverse primer 5'-GTATGTATCTCGAGCTAGTAGGCGTTCTCCAGCT-3'. The PCR product was gel purified, digested with *EcoR1*/*Xho*I and ligated with a similarly digested pGEX-4T1 vector to make the plasmid pGEX-SOST.

Expression and purification of sclerostin. 2 litres of LB broth supplemented with ampicillin (50 μg/ml) were inoculated with saturated pGEX-SOST/BL21 (DE3) culture (1/1000 dilution) and grown at 37°C until A_{600} = 0.6. Protein expression was induced by addition of isopropyl-1-thio-β-D-galactopyranoside (0.25 mM), and cultures were incubated at 25 °C for 4 h. After cooling to 4 °C, the cells were harvested by centrifugation and resuspended in buffer A: phosphate buffer saline (PBS; pH 7.4) with protease inhibitors (Complete, Roche Applied Science), 1 g of wet cell pellet/5 ml of buffer). Cells were lysed by sonication (Sonics VibraCell, microtip, 30% power for 10 min (4 s on, 9.9 s off) with ice cooling) and then centrifuged (30 min, 30,000 × *g*), and

the supernatant was filtered (Corning syringe filter, 0.25 μm) and then applied to 5 ml GSTrap HP columns (GE Life Sciences). The 5-ml column was washed with 40 ml of buffer A, then 15 ml Buffer B (50 mM Tris-HCl, pH 8.0, 10 mM reduced glutathione (Calbiochem) to elute the protein. Pure fractions (by SDS-PAGE) were combined, dialysed against PBS and 5 mM β-mercaptoethanol and stored at 4 °C for short term or frozen at –80°C with 20% glycerol for long term storage.

SELEX. The selection of sclerostin binding aptamers relied on magnetic separation with the GST-sclerostin that was immobilised on the glutathione sepharose magnetic beads. The starting point of the selection process was a random degenerate ssDNA library (SelexApt) that was chemically synthesized and HPLC purified. (SelexApt: 5'-CCG TAA TAC GAC TCA CTA TAG GGG AGC TCG GTA CCG AAT TC-(N30)-AAG CTT TGC AGA GAG GAT CCT T-3'). Primers that anneal to the 5'- and 3'-sequences flanking the degenerate region of SelexApt used during the selection and cloning were: "SelexF", 5'-CCG TAA TAC GAC TCA CTA TAG GGG AGC TCG GTA CCG AAT TC-3'; "SelexR", 5'-AAG GAT CCT CTC TGC AAA GCT T-3'; in non-biotinylated and 5'-biotinylated forms, respectively (HPLC purified). Iterative rounds of aptamer selection and amplification during the SELEX process were modified from previous protocols [30, 31]. 1 nmol of DNA library was incubated with GST-sclerostin immobilised on GST magnetic beads in PBS for 30 min at room temperature. The unbound DNA was separated and removed by washing with PBS. The bound sequences were eluted with PBS containing 10 mM reduced glutathione (GSH) and PCR amplified using biotinylated primers. 90 μl of the PCR reaction product containing enriched biotinylated double stranded DNA was equilibrated with 23 μl of 5 M NaCl and 1 mg of M-280 streptavidin magnetic beads (Dynal) for 10 min. Non-biotinylated single-stranded DNA was recovered and dissociated from the immobilized complementary biotinylated strand using 50 μl of 100 mM NaOH for 5 min. 15 cycles were performed with counter selection using immobilised GST magnetic beads at round 3, 6, 9 and 12. During the last round of SELEX, the recovered DNA molecules were PCR amplified using non-biotinylated primers and cloned into pCR-Blunt II TOPO vectors (Invitrogen) and sequenced. Multiple sequence alignment was performed by clustalW2 [32].

Aptamer-enzyme linked binding assay. An enzyme-linked assay to determine binding of biotinylated aptamers to sclerostin was modified from previous protocols [31, 33]. 96 well plates prepacked with glutathione sepharose media (GE healthcare) were coated with 500 ng purified proteins (GST-sclerostin or GST) in 200 μl coating buffer (50 mM Tris-Cl pH 8.5, 100 mM NaCl and 100 mM KCl) for 1.5 hr at room temperature. The wells were washed 4 times with coating buffer. 3' biotinylated oligodeoxynucleotides (Scl 1 to 4 aptamers (Figure 2), thrombin binding aptamer: 5'-GGTTGGTGTGGTTGG-3' and oligodeoxynucleotide 35-mer random sequence: 5'-GAAGGCCGTTCTCAGTGAACAACAAAAACTGCTAG-3') were heated to 90°C and then cooled slowly to room temperature. 50 nM aptamers were incubated with protein in the 96 well plate overnight at 4°C shaking gently. Wells were washed 6 times with 200 μl of coating buffer for each wash 10 min on a plate vortex. Streptavidin horseradish perioxidase (Molecular Probes) was diluted 1:2000 in buffer and 200 μl aliquots applied to each well. Strips were incubated for 30 min at room temperature and washed again as described above. Then, 150 μl of Turbo- 3,3´,5,5´-tetramethylbenzidine (TMB) (Pierce)

was added to each well and incubated for 20 min at room temperature in the dark. The reaction was quenched by addition of 150 μl of 1M H_2SO_4 and the protein bound aptamer-streptavidin complexes were quantified by determining the absorbance at 450 nm using SpectraMax Plus (Molecular Devices).

Isothermal Titration Calorimetry: The binding affinities and binding enthalpies of the aptamers to GST-sclerostin and GST were measured by ITC (MicroCal VP-ITC, MicroCal Inc. Northampton, MA). In a typical ITC experiment, 15 μM GST-sclerostin or 20 μM GST was loaded into the cell with 200 μM aptamers or random sequence in the titrating syringe. GST-sclerostin and GST were dialysed into the PBS buffer containing β-mercaptoethanol using SnakeSkin Dialysis tubing (Pierce) with a MWCO of 10,000. Aptamers used were weighed out as solids and dissolved into the buffer used for protein dialysis. The titration experiments were performed at 25°C with an initial 0.2 μl injection, followed by thirty 1.2 μl injections. The spacing between injections was 200 s. The stirring speed during the titration was 900 rpm. Data were analysed using MicroCal Origin software by fitting to a single-site binding model. Correction for the enthalpy of ligand linear fit from the last three data points of the titration, after the interaction had reached saturation.

Circular Dichroism: Oligonucleotides (10 μM) were resuspended in PBS or Tris-HCl (10 mM, pH 7.5) buffer that contained KCl or NaCl. Samples were heated at 90°C for 5 min, followed by gradual cooling to room temperature. CD spectra were collected on a JASCO J810 spectropolarimeter (JASCO, MD, USA) equipped with a water-jacketed cell holder at 310nm – 210nm, by using 4 scans at 100 nm min^{-1}, 1 s response time, 1 nm bandwidth. Quartz cells with an optical path length of 1 mm were used for the measurement. The scans of the buffer alone were substracted from the average scans for the sample. CD melting curves obtained at wavelength 260 nm allowed an estimation of melting temperature, T_m, the mid-point temperature of the unfolding process.

Stability of aptamers in cells: 1 μM of Scl 2 and 3' inverted thymidine modified Scl 2 aptamers were added to MC3T3-E1 cells at 80% confluency. Cells were grown in 6 well plates and with 2 ml complete medium (minimal essential media (α-MEM), supplemented with 5% FBS, penicillin/Streptomycin and fungizone) at 37°C supplemented with 5% CO_2. At time point indicated, 10 μl of medium was loaded onto urea-PAGE for electrophoresis. Gels were stained with 1:10000 Sybr Gold (Invitrogen) for 20 min and images were taken under UV.

T-cell factor luciferase reporter assay: MC3T3-E1 cells were seeded in 24-well plates and transiently transfected with either 100 ng of TOP-Wnt induced luciferase plasmid or FOP (control plasmid) using Lipofectamine reagent. Wnt3a (800 ng), sclerostin (800 ng) expression vectors were co-transfected when needed. 10 ng of *Renilla* luciferase vector was co-transfected (pRL-SV40; Promega) to correct for transfection efficiency. 6 hr post-transfection, medium (α-MEM, supplemented with 5% FBS) were changed to antibiotics containing medium supplemented with the indicated concentration of aptamers and incubated for a further 24 hr. Cells were lysed with 100 μl of passive lysis buffer and 20 μl was used for analyses. Luciferase assays were performed using Dual-Luciferase Reported system (TM040; Promega) according to the manufacturer's protocol.

RESULTS

Selection of DNA aptamers binding to sclerostin. To identify novel DNA aptamers that bind to sclerostin, a glutathione sepharose magnetic bead-based selection procedure using immobilised GST-sclerostin was employed. A single stranded DNA library containing a 30-nt random core sequence was passed through the immobilised GST-sclerostin on the beads, then binding nucleic acids were eluted with reduced glutathione. Non-specifically bound aptamers were eliminated during a counter-selection step using the magnetic beads bound to GST (Figure 1). Single-stranded DNA pool was recovered by streptavidin-magnetic bead purification. Enrichment of a pool that specifically bound to the sclerostin was observed after 15 rounds of aptamer selection. We sequenced 30 individual aptamer clones, and observed that 90% of the selected sequences belonged to four related guanosine rich sequences (Figure 2). Notably, aptamers Scl 1 and Scl 2 were dominant sequences that accounted for 80% of the total pool. A high level of sequence homology was observed, with a conserved motif present in almost all clones at approximately the same location in the random region (5'-GGXGGXXGGXTGGG-3'). This stretch of nucleotides may be folded into an unusual guanosine quadruplex structure based on the guanine quartet, which should contribute substantial stability to the overall structure [34].

Binding of selected aptamers to sclerostin. To make an initial measurement of the relative binding affinities of the aptamers to sclerostin, we employed an enzyme-linked solid phase assay whereby the GST-sclerostin was immobilised on a plate then biotinylated aptamers were bound at different concentrations and quantified by enzyme-linked immunoassay [31, 33]. We observed that all the sclerostin aptamers Scl 1-4 bound to GST-sclerostin whilst they did not bind to GST alone as a control (Figure 3). The GST control showed that our counter-selection strategy of using immobilised GST during the selection was effective in removing aptamers that might recognise GST. Scl 3 appeared to bind slightly less potently than the other three aptamers: Scl 1, Scl 2 and Scl 4. Furthermore, the established thrombin binding aptamer was used as a second control for non-specific binding of G quadruplex aptamers to sclerostin and no binding was observed. We therefore concluded that the aptamers specifically bound to GST-sclerostin without binding to GST. The concentrations used in the experiment suggested nanomolar affinity but as this was an immobilised assay we subsequently followed this up with isothermal titration calorimetry to accurately measure the binding affinity in solution.

Aptamer stabilisation and inhibition of sclerostin function in mammalian cells. Natural phosphodiester oligonucleotides are susceptible to degradation by nucleases, and thus would be unsuitable for use in cell studies. Capping the 3' end is one commonly used approach to block 3' to 5' exonuclease attack. Therefore, the stability of sclerostin aptamer (Scl 2) modified with 3' inverted thymidine (3'-InT) was evaluated in MC3T3-E1 cells that were supplemented with 5% FBS (Figure 4A). MC3T3-E1 cells are an osteoblastic cell line that express the receptors upon which sclerostin exert its effect. Without any modifications, aptamers were quickly degraded by nuclease in serum as

observed by the smear (Figure 4A). However, the modified 3' inverted thymidine aptamers were stable with apparent levels unchanged after 28 hr, suggesting that 3' inverted thymidine capping is a suitable approach for the stabilisation of sclerostin aptamers.

To investigate whether the selected 3' InT modified aptamers are able to inhibit sclerostin function in cell culture, we employed lymphoid enhancer factor/T-cell factor (LEF/TCF) luciferase reporter assay to study the effects of aptamers on Wnt mediated activity in osteoblast MC3T3-E1 cells. MC3T3-E1 cells do not endogenously express sclerostin but they do express the receptors and the signalling pathway downstream from sclerostin. Both LEF and TCF are nuclear transducers of an activated canonical Wnt/β-catenin pathway as they interact with β-catenin (Figure 4B). TOP flash luciferase reporter contains three Wnt-specific binding sites for TCF/LEF transcription factors and the firefly luciferase reporter (F*luc*) under the control of herpes simplex virus thymidine kinase; whilst the FOP flash construct is identical to the TOP construct with three TCF binding sites that are mutated and thus serves as a negative control. The luciferase gene is driven by the promoter which is specifically activated by the binding of β-catenin through the activation of Wnt.

The Wnt pathway only becomes active when Wnt3a is expressed (Figure 4C, bars 1 and 2). As expected when both sclerostin and Wnt3a are expressed then sclerostin antagonises the Wnt pathway (Figure 4C, bar 3). The impact of each aptamer was then determined by adding the 3' inverted thymidine modified aptamers at 1.5 μM concentration 6 hours post-transfection, then determining the luciferase activity after a further 24 hours incubation. It was clear that Scl 2 potently inhibited sclerostin's antagonist effect on Wnt signalling (Figure 4C, bar 5) whilst the other three aptamers Scl 1, Scl 3 and Scl 4 were not able to inhibit sclerostin (Figure 4C, bars 4, 6, 7). In further controls, the aptamers did not have any effect on luciferase activity in the absence of Wnt3a and/or SOST, and nor did SOST have any effect in the absence of Wnt3a. Finally, we determined whether the 3' inverted thymidine Scl 2 aptamer showed a dose-response by investigating its impact at varying concentrations from 0.1 μM to 1.5 μM. A clear dose response was observed (Figure 4D) with increasing concentrations of Scl 2 sclerostin inverted thymidine modified aptamer with an IC_{50} of approximately 900 nM.

Sclerostin-Scl 2 aptamer interaction analysis by isothermal titration calorimetry. Our previous binding experiment showed all sclerostin aptamers to have high binding affinity for sclerostin, but concomitant experiments in mammalian cell culture indicated that Scl 2 was the most promising of these aptamers. We performed isothermal titration calorimetry (ITC) to compare the sclerostin aptamers to understand the relationship between affinity and potency against sclerostin. For the ITC experiment, the sclerostin aptamers were titrated into the GST-sclerostin and the heat changes were observed (Figure 5A). Binding isotherms (typical data shown for Scl2 binding to sclerostin) for the interaction showed an exothermic binding event (Figure 5A), and controls showed that a random DNA sequence was unable to bind GST-sclerostin (Figure 5B) and that the

aptamer was binding to sclerostin and not the GST domain of the GST-sclerostin fusion (Figure 5C).

Our results showed that the binding stoichiometry (n) was 0.91 ± 0.02, indicating that ~0.91 molecules of Scl 2 aptamer bind per one sclerostin molecule. Binding of Scl 2 aptamer to sclerostin was exothermic. Binding is enthalpically favored but entropically opposed (Table 1). The large enthalpic contribution to the ΔG of binding between aptamers and GST-sclerostin implies the formation of hydrogen bonds and electrostatic interactions.

The thermodynamic parameters of sclerostin aptamers 1 to 4 and Scl 2 3' inverted thymidine aptamer binding to GST-SOST derived from ITC are summarised (Table 1). All aptamers bound to sclerostin with affinities with a K_D ranging from 0.2-2.1 μM. Scl 2 aptamers and its inverted thymidine modified form which showed potency in mammalian cell culture bound to GST-SOST more strongly than Scl 1 and Scl 3. Consistent with the previous enzyme-linked binding assay, Scl 4 also bound tightly to GST-SOST. Although Scl 4 has higher binding affinity than Scl 2, Scl 4 did not have an inhibitory effect on sclerostin in cell culture. Considering that Scl 2 has a 5' "tail" whilst Scl 4 has a 3' "tail", this indicates that the 5' "tail" on Scl 2 may also be important for efficacy in cell culture.

Biophysical properties of sclerostin aptamers by circular dichroism. To characterise the secondary structure of the sclerostin aptamers, we employed circular dichroism to experimentally investigate whether G-quadruplex structure was formed. In the CD spectra, all sclerostin aptamers showed a positive maximum peak near 265 nm in PBS (Figure 6A). A peak at 265 nm is spectroscopic criteria for aptamers to have parallel G-quadruplex structure [34]. Dependence of G-quadruplex formation on metal ion coordination, particularly potassium ions, has been previously reported [35]. The Scl 2 aptamers in Na^+ and K^+ showed similar CD spectra. With a decrease in K^+ concentration (100mM to 1mM), the ellipticity of the 265 nm peaks was almost the same. However, the extent of G-quadruplex formation was slightly affected in the absence of potassium ions (Figure 6B). Furthermore, we determined the thermal stability of the G-quadruplex structure of aptamer Scl 2 by observing circular dichroism under varying temperature, thus determining the T_m value of aptamer Scl 2 to be 75°C (Figure 6C). This suggested that the structure is stable and suitable for application in the cellular environment.

DISCUSSION

This study identifies a DNA aptamer that binds specifically to sclerostin with nanomolar affinity. The aptamer had parallel G quadruplex characteristics, was thermally stable, and could be stabilised to nuclease activity by 3' inverted thymidine capping. The stabilised aptamer potently inhibited sclerostin's antagonistic effect on Wnt signalling in a cell culture assay showing a dose-response with an IC_{50} of 900 nM.

With particular relevance to this study, the NMR structure of sclerostin was published by two independent groups recently [8, 36]. One study revealed that sclerostin has a binding site for heparin, and that the antibody binding site and heparin binding site

on sclerostin had minimal overlap [8]. The second study highlighted the unusual abundance of positively charged residues resulting in a basic protein (pI_{calc} 9.6) [36]. Calculation of the electrostatic potential between sclerostin and LRP5 propellor revealed the positively charged putative binding site of sclerostin bound directly to the highly negatively charged binding site on LRP5 [36]. In the selection of aptamers in this study, it is likely that negatively charged phosphodiester backbone in the aptamers would be selected against the major positively charged surface on sclerostin. This would also be consistent with the highly enthalpic contributions observed in our ITC experiments in the interaction between the sclerostin and the aptamer. Thus, the Scl 2 aptamer may act as an LRP 5 mimic and directly compete for binding with LRP5. Alternatively, the aptamers may mimic heparin and compete for heparin binding, thus disrupting the heparin-mediated localisation of sclerostin to the cell surface [8]. Further experiments would be required to test these alternate hypotheses. As the antibody binding site had little overlap with the heparin binding site [8], it is possible that the aptamer binds at a site distinct from the antibody binding site, thus suggesting that an aptamer/antibody cocktail may have a synergistic effect on inhibiting sclerostin function.

The relative potencies of the established monoclonal antibodies compared to the aptamer in this study can be compared. A similar assay was performed in MC3T3-E1 cells to investigate the potency of antibodies inhibiting sclerostin function using an antibody concentration of 100 μg/ml, to totally inhibit sclerostin function although the IC_{50} was not disclosed [8]. In our experiments we used a sclerostin aptamer concentration of 1.5 μM, equivalent to 14.2 μg/ml, to inhibit sclerostin, so the potency in cell culture could be considered to be in a similar range. As far as we are aware, the dissociation constants of the specific monoclonal antibodies that went into animal and human trials have not been disclosed. However, monoclonal antibodies against the N-terminal and C-terminal regions of human and mouse sclerostin peptides in another study bound tighter with K_D of 3 nM for an antibody against the N-terminal peptide and 8 nM for an antibody against the C-terminal peptide [37], compared to 700 nM for Scl 2 herein. Nevertheless, further optimization and modification of Scl 2 would be likely to increase its affinity several-fold as has been performed in other aptamer studies [25].

Targeting sclerostin to stimulate bone growth is now established as an approach with significant therapeutic potential given the pioneering studies using monoclonal antibodies [24]. One potential drawback of targeting Wnt signalling is that the Wnt signalling is not an on-off process [24]. If the Wnt signalling is constitutively activated, cancer may result, and conversely if Wnt signalling is fully inhibited, osteoporosis and heart failure may result [24]. This suggests that fine-tuning by using, for example, aptamer antidotes based on complementary base-pairing [38, 39] could provide an approach to control anti-sclerostin activity which would not be available for antibody-based therapy and small molecules. Nevertheless, aptamers can have drawbacks in that their pharmacokinetic and systemic properties are variable and can be unpredictable, and their therapeutic use is less established than antibodies [25]. Further research will be required to assess aptamer efficacy in animal models to investigate how aptamer-based targeting compares to antibody-based targeting, and whether there is any potential for a synergistic approach. Further optimisation and modification of this particular aptamer may lead to the development of a new bone-forming agent.

ACKNOWLEDGEMENTS

This research was funded by the Hong Kong Research Grants Council (RGC) under the General Research Fund scheme HKU 7488/06M. We thank Prof. Wong Kam Po (Department of Biochemistry, The Chinese University of Hong Kong) for access to the circular dichroism spectropolarimeter.

REFERENCES

1. Balemans, W., Ebeling, M., Patel, N., Van Hul, E., Olson, P., Dioszegi, M., Lacza, C., Wuyts, W., Van Den Ende, J., Willems, P., Paes-Alves, A. F., Hill, S., Bueno, M., Ramos, F. J., Tacconi, P., Dikkers, F. G., Stratakis, C., Lindpaintner, K., Vickery, B., Foernzler, D., and Van Hul, W. (2001) Increased bone density in sclerosteosis is due to the deficiency of a novel secreted protein (SOST). Hum. Mol. Genet. **10**, 537-543.
2. Brunkow, M. E., Gardner, J. C., Van Ness, J., Paeper, B. W., Kovacevich, B. R., Proll, S., Skonier, J. E., Zhao, L., Sabo, P. J., Fu, Y., Alisch, R. S., Gillett, L., Colbert, T., Tacconi, P., Galas, D., Hamersma, H., Beighton, P., and Mulligan, J. (2001) Bone dysplasia sclerosteosis results from loss of the SOST gene product, a novel cystine knot-containing protein. Am. J. Hum. Genet. **68**, 577-589.
3. Hamersma, H., Gardner, J., and Beighton, P. (2003) The natural history of sclerosteosis. Clin. Genet. **63**, 192-197.
4. Piters, E., Culha, C., Moester, M., Van Bezooijen, R., Adriaensen, D., Mueller, T., Weidauer, S., Jennes, K., De Freitas, F., Lowik, C., Timmermans, J. P., Van Hul, W., and Papapoulos, S. (2010) First missense mutation in the SOST gene causing sclerosteosis by loss of sclerostin function. Hum. Mutat. **31**, E1526-1543.
5. Paszty, C., Turner, C. H., and Robinson, M. K. (2010) Sclerostin: a gem from the genome leads to bone-building antibodies. J. Bone Miner. Res. **25**, 1897-1904.
6. Agholme, F., Li, X., Isaksson, H., Ke, H. Z., and Aspenberg, P. (2010) Sclerostin antibody treatment enhances metaphyseal bone healing in rats. J. Bone Miner. Res. **25**, 2412-2418.
7. Padhi, D., Jang, G., Stouch, B., Fang, L., and Posvar, E. (2010) Single-dose, placebo-controlled, randomized study of AMG 785, a sclerostin monoclonal antibody. J. Bone Miner. Res., accepted.
8. Veverka, V., Henry, A. J., Slocombe, P. M., Ventom, A., Mulloy, B., Muskett, F. W., Muzylak, M., Greenslade, K., Moore, A., Zhang, L., Gong, J., Qian, X., Paszty, C., Taylor, R. J., Robinson, M. K., and Carr, M. D. (2009) Characterization of the structural features and interactions of sclerostin: molecular insight into a key regulator of Wnt-mediated bone formation. J. Biol. Chem. **284**, 10890-10900.
9. Van Bezooijen, R. L., Papapoulos, S. E., and Lowik, C. W. (2005) Bone morphogenetic proteins and their antagonists: the sclerostin paradigm. J. Endocrinol. Invest. **28**, 15-17.
10. Winkler, D. G., Sutherland, M. K., Geoghegan, J. C., Yu, C., Hayes, T., Skonier, J. E., Shpektor, D., Jonas, M., Kovacevich, B. R., Staehling-Hampton, K., Appleby, M., Brunkow, M. E., and Latham, J. A. (2003) Osteocyte control of bone formation via sclerostin, a novel BMP antagonist. EMBO J. **22**, 6267-6276.
11. Li, X., Zhang, Y., Kang, H., Liu, W., Liu, P., Zhang, J., Harris, S. E., and Wu, D. (2005) Sclerostin binds to LRP5/6 and antagonizes canonical Wnt signaling. J. Biol. Chem. **280**, 19883-19887.
12. Kamiya, N., Ye, L., Kobayashi, T., Mochida, Y., Yamauchi, M., Kronenberg, H. M., Feng, J. Q., and Mishina, Y. (2008) BMP signaling negatively regulates bone

mass through sclerostin by inhibiting the canonical Wnt pathway. Development **135**, 3801-3811.

13. Ten Dijke, P., Krause, C., De Gorter, D. J., Lowik, C. W., and Van Bezooijen, R. L. (2008) Osteocyte-derived sclerostin inhibits bone formation: its role in bone morphogenetic protein and Wnt signaling. J. Bone Joint Surg. Am. **90 Suppl 1**, 31-35.
14. Van Bezooijen, R. L., Roelen, B. A., Visser, A., Van der Wee-Pals, L., De Wilt, E., Karperien, M., Hamersma, H., Papapoulos, S. E., Ten Dijke, P., and Lowik, C. W. (2004) Sclerostin is an osteocyte-expressed negative regulator of bone formation, but not a classical BMP antagonist. J. Exp. Med. **199**, 805-814.
15. Semenov, M., Tamai, K., and He, X. (2005) SOST is a ligand for LRP5/LRP6 and a Wnt signaling inhibitor. J. Biol. Chem. **280**, 26770-26775.
16. Gong, Y., Slee, R. B., Fukai, N., Rawadi, G., Roman-Roman, S., Reginato, A. M., Wang, H., Cundy, T., Glorieux, F. H., Lev, D., et al. (2001) LDL receptor-related protein 5 (LRP5) affects bone accrual and eye development. Cell **107**, 513-523.
17. Boyden, L. M., Mao, J., Belsky, J., Mitzner, L., Farhi, A., Mitnick, M. A., Wu, D., Insogna, K., and Lifton, R. P. (2002) High bone density due to a mutation in LDL-receptor-related protein 5. N. Engl. J. Med. **346**. 1513-1521.
18. Li, X., Ominsky, M. S., Warmington, K. S., Morony, S., Gong, J., Cao, J., Gao, Y., Shalhoub, V., Tipton, B., Haldankar, R., et al. (2009) Sclerostin antibody treatment increases bone formation, bone mass, and bone strength in a rat model of postmenopausal osteoporosis. J. Bone Miner. Res. **24**, 578-588.
19. Eddleston, A., Marenzana, M., Moore, A. R., Stephens, P., Muzylak, M., Marshall, D., and Robinson, M. K. (2009) A short treatment with an antibody to sclerostin can inhibit bone loss in an ongoing model of colitis. J. Bone Miner. Res. **24**, 1662-1671.
20. Ominsky, M. S., Vlasseros, F., Jolette, J., Smith, S. Y., Stouch, B., Doellgast, G., Gong, J., Gao, Y., Cao, J., Graham, K., Tipton, B., Cai, J., Deshpande, R., Zhou, L., Hale, M. D., Lightwood, D. J., Henry, A. J., Popplewell, A. G., Moore, A. R., Robinson, M. K., Lacey, D. L., Simonet, W. S., and Paszty, C. (2010) Two doses of sclerostin antibody in cynomolgus monkeys increases bone formation, bone mineral density, and bone strength. J. Bone Miner. Res. **25**, 948-959.
21. Tian, X., Setterberg, R. B., Li, X., Paszty, C., Ke, H. Z., and Jee, W. S. (2010) Treatment with a sclerostin antibody increases cancellous bone formation and bone mass regardless of marrow composition in adult female rats. Bone. **47**, 529-533.
22. Agholme, F., Li, X., Isaksson, H., Ke, H. Z., and Aspenberg, P. (2010) Sclerostin antibody treatment enhances metaphyseal bone healing in rats. J. Bone Miner. Res. **25**, 2412-2418.
23. Paszty, C., Turner, C. H., and Robinson, M. K. (2010) Sclerostin: A gem from the genome leads to bone building antibodies. J. Bone Miner. Res. **25**, 1897-1904.
24. Rey, J. P., and Ellies, D. L. (2010) Wnt modulators in the biotech pipeline. Dev. Dyn. **239**, 102-114.
25. Keefe, A. D., Pai, S., and Ellington, A. (2010) Aptamers as therapeutics. Nat Rev Drug Discov. **9**, 537-550.

26. Tuerk, C., and Gold, L. (1990) Systematic evolution of ligands by exponential enrichment: RNA ligands to bacteriophage T4 DNA polymerase. Science **249**, 505-510.
27. Ellington, A. D., and Szostak, J. W. (1990) In vitro selection of RNA molecules that bind specific ligands. Nature **346**, 818-822.
28. Que-Gewirth, N. S., and Sullenger, B. A. (2007) Gene therapy progress and prospects: RNA aptamers. Gene Ther. **14**, 283-291.
29. Ruckman, J., Green, L. S., Beeson, J., Waugh, S., Gillette, W. L., Henninger, D. D., Claesson-Welsh, L., and Janjic, N. (1998) 2'-Fluoropyrimidine RNA-based aptamers to the 165-amino acid form of vascular endothelial growth factor (VEGF165). Inhibition of receptor binding and VEGF-induced vascular permeability through interactions requiring the exon 7-encoded domain. J. Biol. Chem. **273**, 20556-20567.
30. Shum, K. T., and Tanner, J. A. (2008) Differential inhibitory activities and stabilisation of DNA aptamers against the SARS coronavirus helicase. Chembiochem **9**, 3037-3045.
31. Murphy, M. B., Fuller, S. T., Richardson, P. M., and Doyle, S. A. (2003) An improved method for the in vitro evolution of aptamers and applications in protein detection and purification. Nucleic Acids Res. **31**, e110.
32. Larkin, M. A., Blackshields, G., Brown, N. P., Chenna, R., McGettigan, P. A., McWilliam, H., Valentin, F., Wallace, I. M., Wilm, A., Lopez, R., Thompson, J. D., Gibson, T. J., and Higgins, D. G. (2007) Clustal W and Clustal X version 2.0. Bioinformatics **23**, 2947-2948.
33. Choi, M. Y., Chan, C. C., Chan, D., Luk, K. D., Cheah, K. S., and Tanner, J. A. (2009) Biochemical consequences of sedlin mutations that cause spondyloepiphyseal dysplasia tarda. Biochem. J. **423**, 233-242.
34. Shafer, R. H., and Smirnov, I. (2000) Biological aspects of DNA/RNA quadruplexes. Biopolymers **56**, 209-227.
35. Burge, S., Parkinson, G. N., Hazel, P., Todd, A. K., and Neidle, S. (2006) Quadruplex DNA: sequence, topology and structure. Nucleic Acids Res. **34**, 5402-5415.
36. Weidauer, S. E., Schmieder, P., Beerbaum, M., Schmitz, W., Oschkinat, H., and Mueller, T. D. (2009) NMR structure of the Wnt modulator protein Sclerostin. Biochem. Biophys. Res. Commun. **380**, 160-165.
37. Craig, T. A., Sommer, S. L., Beito, T. G., and Kumar, R. (2009) Production and characterization of monoclonal antibodies to human sclerostin. Hybridoma (Larchmt) **28**, 377-381.
38. Oney, S., Lam, R. T., Bompiani, K. M., Blake, C. M., Quick, G., Heidel, J. D., Liu, J. Y., Mack, B. C., Davis, M. E., Leong, K. W., and Sullenger, B. A. (2009) Development of universal antidotes to control aptamer activity. Nat. Med. **15**, 1224-1228.
39. Rusconi, C. P., Roberts, J. D., Pitoc, G. A., Nimjee, S. M., White, R. R., Quick, G., Jr., Scardino, E., Fay, W. P., and Sullenger, B. A. (2004) Antidote-mediated control of an anticoagulant aptamer in vivo. Nat. Biotechnol. **22**, 1423-1428.

Aptamers	K_D (μM)	ΔH (kcal/mol)	TΔS (kcal/mol)	ΔG (kcal/mol)
Scl 1	1.34 ± 0.33	-27.1 ± 2.1	-19.1 ± 2.2	-8.0 ± 0.2
Scl 2	0.67 ± 0.08	-18.6 ± 2.1	-10.2 ± 2.2	-8.4 ± 0.1
Scl 3	2.07 ± 0.68	-24.3 ± 5.9	-16.6 ± 6.1	-7.7 ± 0.2
Scl 4	0.20 ± 0.05	-25.2 ± 2.1	-16.1 ± 2.2	-9.1 ± 0.1
Scl 2 InT	0.41 ± 0.03	-18.3 ± 1.7	-8.2 ± 1.9	-10.1 ± 0.2

Table 1: Experimentally determined thermodynamic parameters for sclerostin aptamers binding to GST-sclerostin derived from ITC measurements at 25 °C.

FIGURE LEGENDS

Figure 1. A schematic drawing showing the method used for sclerostin aptamer selection. GST-tagged sclerostin was immobilised on magnetic beads. The library was incubated with the target beads for binding. Unbound oligonucleotides were washed away, and the bound ones were eluted with the target by reduced glutathione. The selected binders were amplified by PCR by using biotinylated primers. ssDNA was subsequently purified from the PCR product using streptavidin coated magnetic beads, resulting in an enriched DNA pool, which was used in the next SELEX round. After the last round, the selected aptamers were cloned, sequenced and characterised. Counter selections were performed using GST immobilized magnetic beads.

Figure 2. Aptamer selection results. Sequences of the aptamers that were isolated from the ssDNA pool after 15 rounds of selection against GST-sclerostin. Conserved nucleotides are marked by an asterisk.

Figure 3. Determination of relative binding strength of aptamers against sclerostin using an aptamer enzyme-linked assay. Combinations of sclerostin aptamers, thrombin binding aptamers, GST-sclerostin and GST protein (indicated by plus signs below the graph) were evaluated for their binding activity and cross-reactivity. Data shown are the mean values of three assay points (± SEM).

Figure 4. Aptamer stabilisation and inhibition of sclerostin function in mammalian cells. A.) Stability assay on unmodified Scl 2 aptamers and 3' inverted thymidine modified Scl 2 aptamers. B.) Schematic showing the principles behind the reporter luciferase activity assay. C.) Effect of 3' inverted thymidine modified sclerostin aptamers on Wnt3a mediated activity in MC3T3-E1 cells. Data shown are the mean values of three assay points (± SEM). *** represents values statistically significantly different by unpaired t-test with 95% confidence. D.) Effect of varying concentrations of 3' inverted thymidine modified Scl 2 aptamers against sclerostin function. Data shown are the mean values of three assay points (± SEM).

Figure 5. Aptamer-sclerostin interaction analysis by ITC. Raw calorimetric data and binding isotherm of the interaction of aptamers and protein are shown in upper and lower panel respectively. A.) ITC analysis of the binding of Scl 2 aptamer to GST-sclerostin. (i) Titration of Scl 2 aptamers into PBS buffer. (ii) Titration of Scl 2 aptamer into GST-sclerostin. B.) Titration of random sequence into GST-sclerostin. C.) Titration of Scl 2 aptamer into GST.

Figure 6. **Secondary structure analysis of aptamer structure by CD.** A.) CD spectra of sclerostin aptamers, 35-mer random sequence and thrombin binding aptamer in PBS. B.) CD spectra of Scl 2 aptamer in different buffer conditions. C.) CD melting spectra of Scl 2 aptamers.

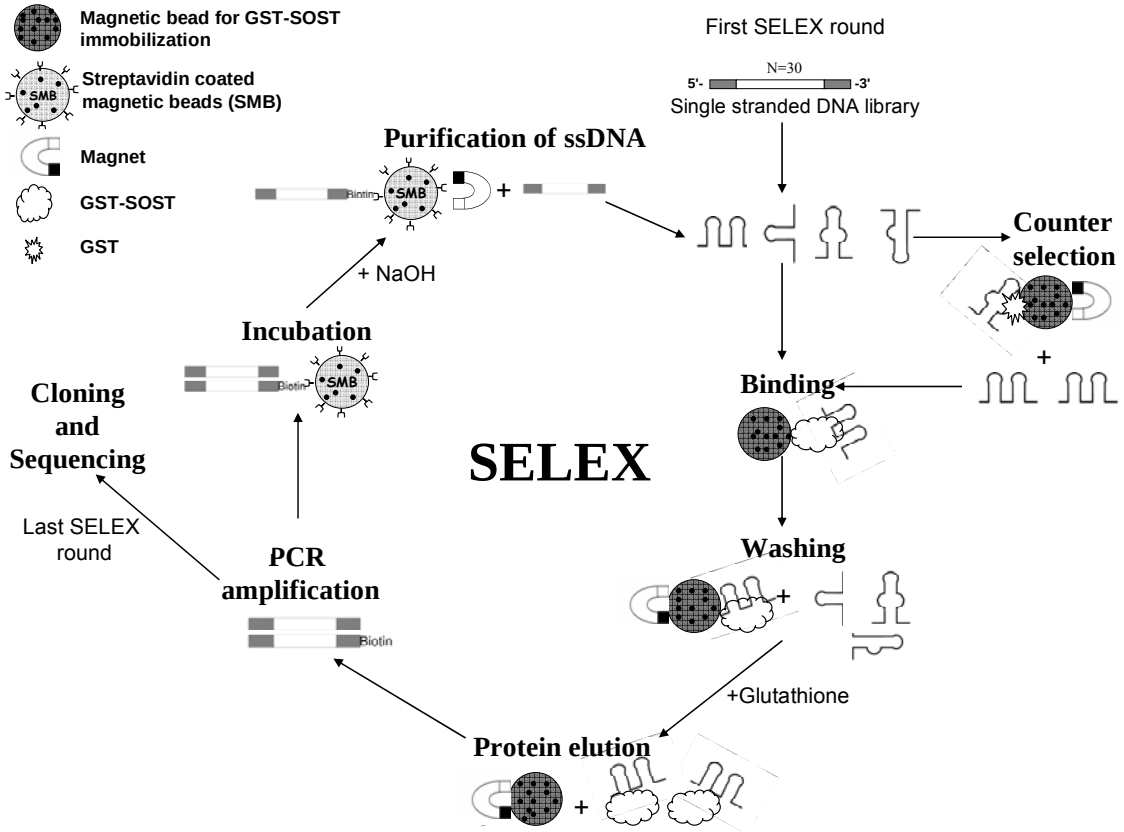
Magnetic bead for GST-SOST immobilization
Streptavidin coated magnetic beads (SMB)
Magnet
GST-SOST
GST
First SELEX round
N=30
5'-
-3'
Single stranded DNA library
Purification of ssDNA
Biotin
SMB
+
+ NaOH
Incubation
Counter selection
Binding
Cloning and Sequencing
SELEX
Last SELEX round
PCR amplification
Washing
+Glutathione
Protein elution

Figure 1

Aptamer clone	Core region of the aptamer sequences (5' to 3')	No. of nucleotides	Percentage
	** ** ** ****		
Scl 1	GTTTCCAAAGCCGGGGGGGTGGGATGGGTT----------	30	56%
Scl 2	TTGCGCGTTAATTGGGGGGGTGGGTGGGTT----------	30	24%
Scl 3	TGCCTTGTTATTGTGGTGGGCGGGTGGGAC----------	30	7%
Scl 4	----------GGGGGGGGTGGGGTGGGTCAATATTCTCGTC	31	3%
Other Sequences			10%

Figure 2

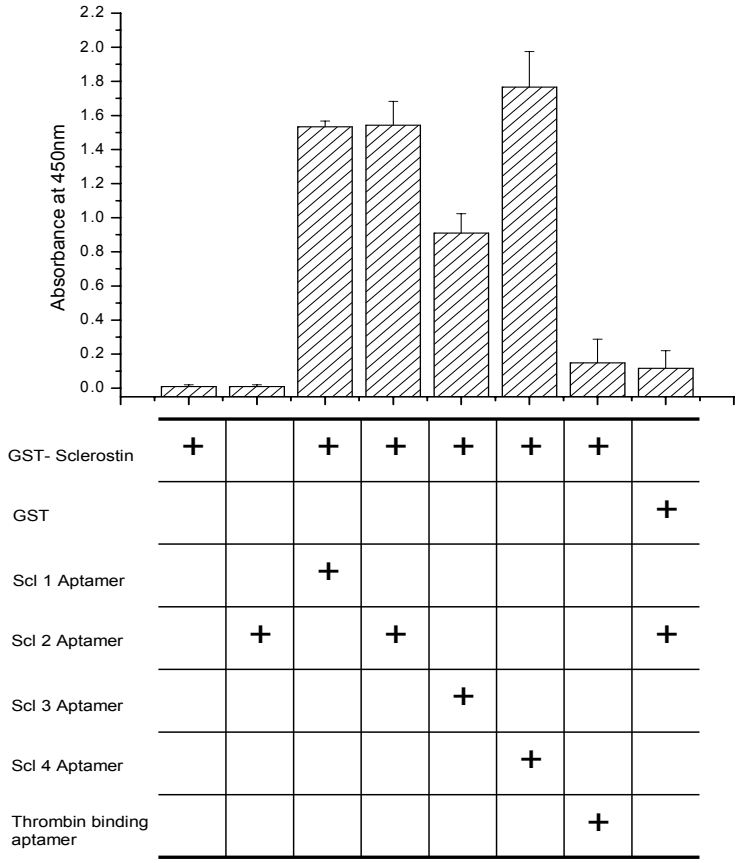
Absorbance at 450nm
2.2
2.0
1.8
1.6
1.4
1.2
1.0
0.8
0.6
0.4
0.2
0.0
GST- Sclerostin
GST
Scl 1 Aptamer
Scl 2 Aptamer
Scl 3 Aptamer
Scl 4 Aptamer
Thrombin binding aptamer

Figure 3

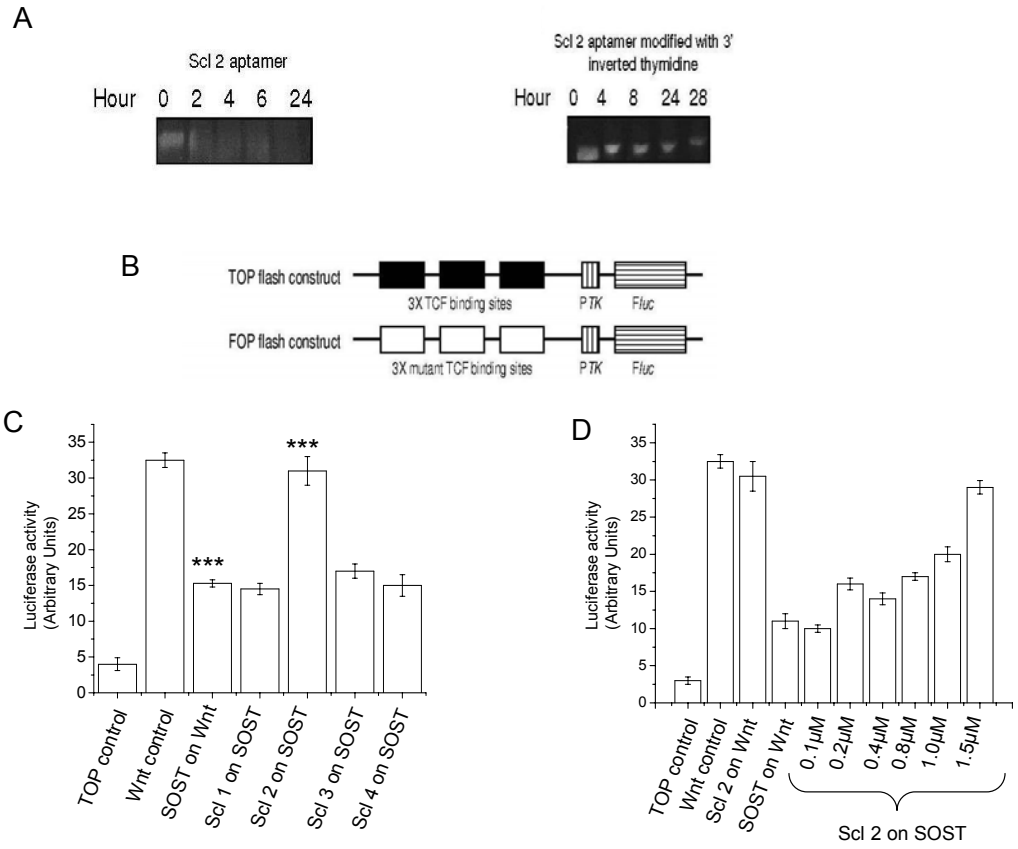
A
Scl 2 aptamer
Hour 0 2 4 6 24
Scl 2 aptamer modified with 3' inverted thymidine
Hour 0 4 8 24 28
B
TOP flash construct
3X TCF binding sites
PTK
Fluc
FOP flash construct
3X mutant TCF binding sites
PTK
Fluc
C
Luciferase activity (Arbitrary Units)
***
***
TOP control
Wnt control
SOST on Wnt
Scl 1 on SOST
Scl 2 on SOST
Scl 3 on SOST
Scl 4 on SOST
D
Luciferase activity (Arbitrary Units)
TOP control
Wnt control
Scl 2 on Wnt
SOST on Wnt
0.1μM
0.2μM
0.4μM
0.8μM
1.0μM
1.5μM
Scl 2 on SOST

Figure 4

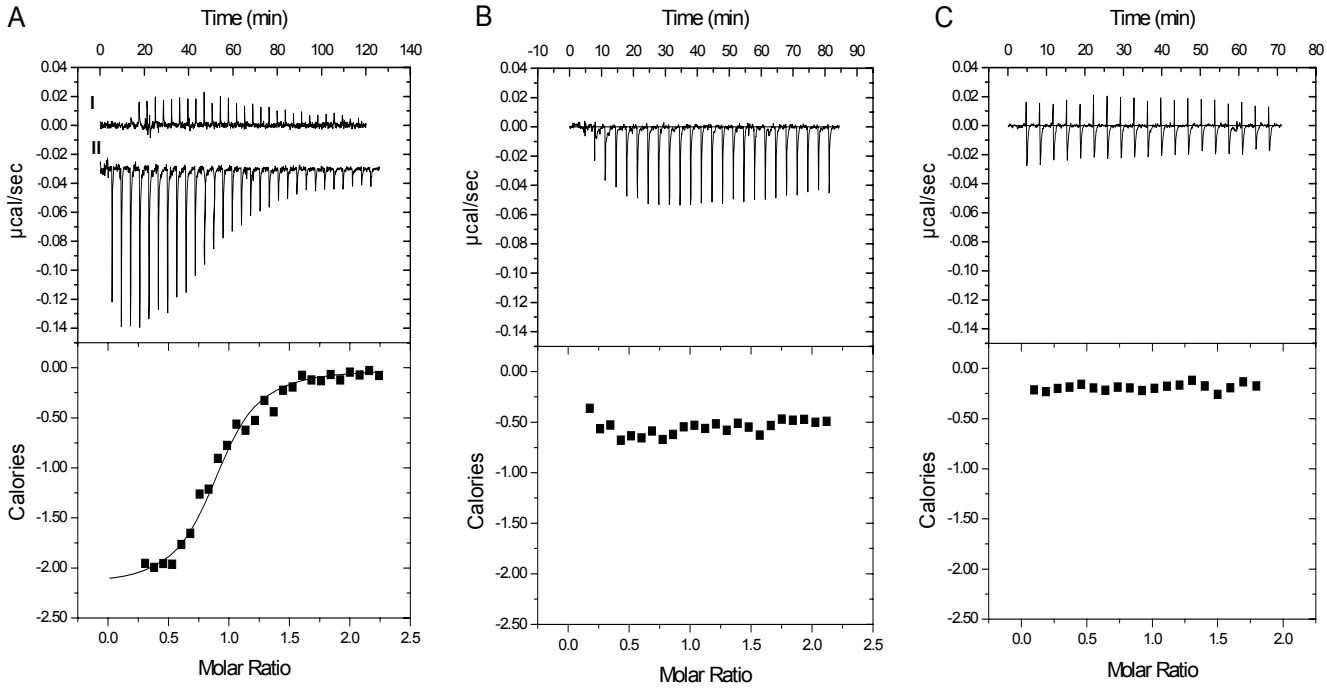
A
Time (min)
µcal/sec
Calories
Molar Ratio
I
II
B
Time (min)
µcal/sec
Calories
Molar Ratio
C
Time (min)
µcal/sec
Calories
Molar Ratio

Figure 5

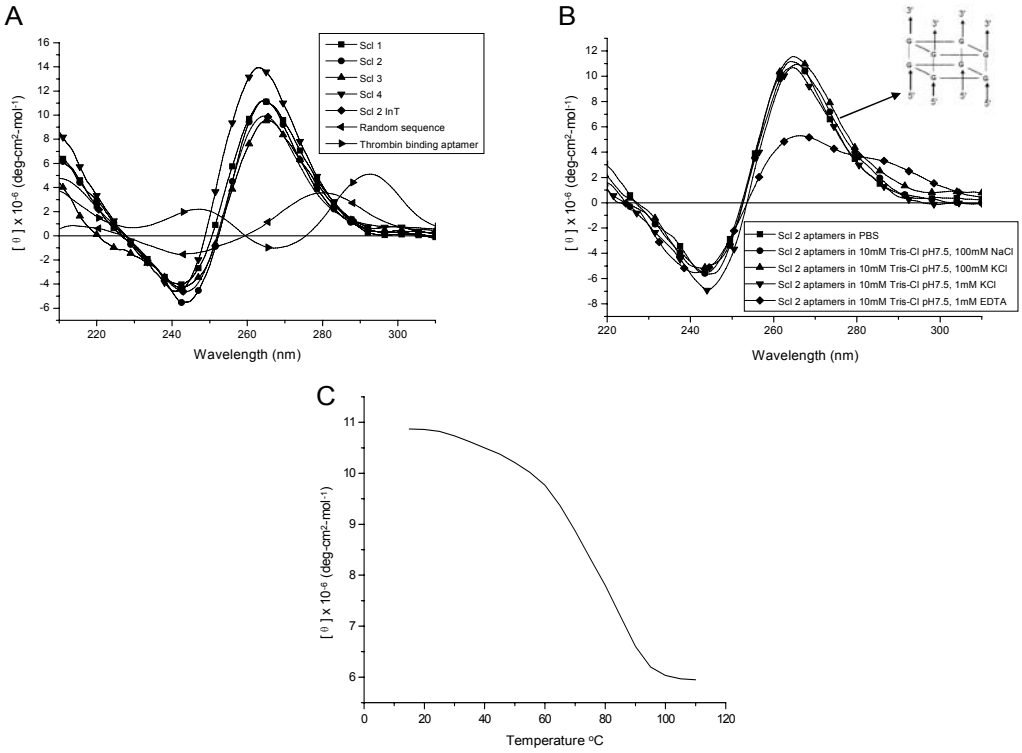
A
Scl 1
Scl 2
Scl 3
Scl 4
Scl 2 InT
Random sequence
Thrombin binding aptamer
[θ] x 10-6 (deg-cm2-mol-1)
Wavelength (nm)
B
Scl 2 aptamers in PBS
Scl 2 aptamers in 10mM Tris-Cl pH7.5, 100mM NaCl
Scl 2 aptamers in 10mM Tris-Cl pH7.5, 100mM KCl
Scl 2 aptamers in 10mM Tris-Cl pH7.5, 1mM KCl
Scl 2 aptamers in 10mM Tris-Cl pH7.5, 1mM EDTA
[θ] x 10-6 (deg-cm2-mol-1)
Wavelength (nm)
C
[θ] x 10-6 (deg-cm2-mol-1)
Temperature oC

Figure 6